



HAL
open science

Biocompatible fluorenylphthalocyanines for one- and two-photon photodynamic therapy and fluorescence imaging

Seifallah Abid, Christophe Nguyen, Morgane Daurat, Denis Durand, Bassem Jamoussi, Mireille Blanchard-desce, Magali Gary-Bobo, Olivier Mongin, Christine O. Paul-Roth, Frédéric Paul

► **To cite this version:**

Seifallah Abid, Christophe Nguyen, Morgane Daurat, Denis Durand, Bassem Jamoussi, et al.. Biocompatible fluorenylphthalocyanines for one- and two-photon photodynamic therapy and fluorescence imaging. *Dyes and Pigments*, 2022, 197, pp.109840. 10.1016/j.dyepig.2021.109840 . hal-03870905

HAL Id: hal-03870905

<https://hal.science/hal-03870905v1>

Submitted on 18 Jan 2023

HAL is a multi-disciplinary open access archive for the deposit and dissemination of scientific research documents, whether they are published or not. The documents may come from teaching and research institutions in France or abroad, or from public or private research centers.

L'archive ouverte pluridisciplinaire **HAL**, est destinée au dépôt et à la diffusion de documents scientifiques de niveau recherche, publiés ou non, émanant des établissements d'enseignement et de recherche français ou étrangers, des laboratoires publics ou privés.



Distributed under a Creative Commons Attribution 4.0 International License

Biocompatible fluorenylphthalocyanines for one and two-photon photodynamic therapy and fluorescence imaging

Seifallah Abid,^{a,d} Christophe Nguyen,^b Morgane Daurat,^b Denis Durand,^b Bassem Jamoussi,^{d,e} Mireille Blanchard-Desce,^{*,c} Magali Gary-Bobo,^{*,b} Olivier Mongin,^a Christine O. Paul-Roth,^{*,a} Frédéric Paul^{*,a}

^a Univ Rennes, INSA Rennes, CNRS, ISCR (Institut des Sciences Chimiques de Rennes) – UMR 6226, F-35000 Rennes, France. E-mail: christine.paul@univ-rennes1.fr or christine.paul@insa-rennes.fr

^b IBMM, Univ Montpellier, CNRS, ENSCM, Montpellier, France. E-mail: magali.gary-bobo@inserm.fr.

^c Univ. Bordeaux, Institut des Sciences Moléculaires (CNRS UMR 5255), 33405 Talence, France. E-mail: mireille.blanchard-desce@u-bordeaux.fr.

^d Université de Carthage, Faculté des Sciences de Bizerte, Tunisie

^e Department of Environmental Sciences, Faculty of Meteorology, Environment and Arid Land Agriculture, King Abdulaziz University, Jeddah, Saudi Arabia

Abstract: The synthesis and the optical properties of a family of new fluorenyl phthalocyanines substituted with water-solubilizing triethyleneglycol chains is described. These biocompatible molecules exhibit strong one and two-photon absorptions, together with fluorescence and photosensitization properties similar to those of their lipophilic analogs, thus outperforming unsubstituted zinc phthalocyanine in terms of brightness and singlet oxygen production. They were subsequently probed *in vitro* on cancer cells under one and two-photon

excitation in both fluorescence imaging and photodynamic therapy experiments. The metal-free compound was shown to be more biocompatible and thus more promising than the zinc complex for theranostic applications.

Keywords: Phthalocyanine, Fluorene, Two-photon absorption, Oxygen sensitization, Photodynamic Therapy, Fluorescence imaging

Introduction

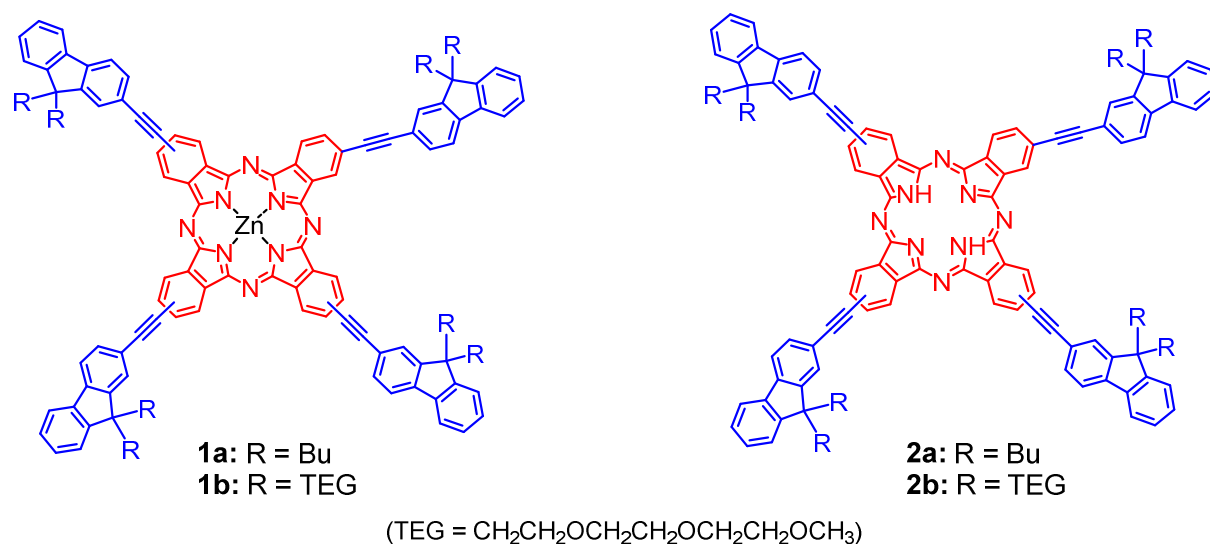
Photodynamic therapy (PDT) is often used for curing various kinds of cancers but also other diseases such as bacterial infections or age-related macular degeneration (AMD).^[1] This therapeutic approach is based on the photoexcitation in the visible or near-infrared range of a photosensitizer (PS) in presence of molecular oxygen ($^3\text{O}_2$) to generate singlet oxygen ($^1\text{O}_2$) and/or other cytotoxic oxygen-based species (ROS) leading eventually to the destruction of the nearby tissues.^[1-2] Targeting can be achieved by specifically functionalizing the PS or by carefully controlling the irradiated tissular region. In this respect, excitation via two-photon absorption (2PA) is quite interesting since it allows an even deeper penetration in tissues than with one-photon absorption (1PA), but also an intrinsic three-dimensional resolution leading to better spatial control of the $^1\text{O}_2$ generation,^[3] particularly adapted for the treatment of small tumors. To be efficient, the PSs have to exhibit very large 2PA cross-sections in the NIR therapeutic windows (NIR1: 700-950 nm and NIR2:1100-1350 nm)^[4] and high singlet oxygen quantum yield and/or ROS production ability.^[5]

While various promising families of photosensitizers have been identified for PDT so far,^[5-6] such as small conjugated organic chromophores substituted with heavy atoms,^[7] transition metal complexes,^[8] large conjugated polymers,^[9] dendrimeric^[10] or doped nanoparticles,^[11]

many among the other photosensitizers often investigated for applicative outcomes possess tetrapyrrolic structures, mostly porphyrins, chlorin and bacteriochlorin derivatives,^[1, 12] but also phthalocyanines (Pcs).^[12-13] Only three (metallo)phthalocyanines are currently engaged in clinical PDT trials: Pc4, Photocyanine and Photosens, coordinated to silicon, zinc and aluminum, respectively. However, phthalocyanines exhibit several advantages over porphyrins, including a lower skin phototoxicity in relation with their lower absorption in the green part of the visible (where sunlight intensity is the highest), and a stronger absorption in the red visible range (> 650 nm) (Q band extinction coefficient of $\sim 2 \times 10^5 \text{ M}^{-1} \text{ cm}^{-1}$), which allows increased penetration depth in tissues.).^[12-13] Moreover, the singlet oxygen quantum yields of (metallo)phthalocyanines^[14] are comparable to those of porphyrins, while exhibiting higher fluorescence quantum yields,^[15] making them appealing for theranostic applications combining imaging and PDT.

Likewise to porphyrins,^{[6],[16]} two-photon excitation of phthalocyanine-based photosensitizers in the near infrared (NIR) range has been reported previously.^[17] While, the 2PA cross-sections in the NIR of current clinical porphyrin (10 GM for Photofrin and 50 GM for Visudyne)^[18] as well as phthalocyanine (70 GM for Photosens)^[17b] PSs are too low for practical use in two-photon PDT (2P-PDT), efforts have been made to develop PSs with enhanced 2PA cross-sections in the NIR1 region, either with a tetrapyrrolic structure or not,^[5-6] but only few of them are actually phthalocyanine derivatives.^[19] Within this context, we have developed porphyrin-,^[20] and more recently phthalocyanine-based systems,^[19j, 21] associating peripheral (linear or dendritic) fluorenyl-based two-photon absorbing antennae and a macrocyclic photosensitizing (and red emitting) core. Following this approach, tetrasubstituted zinc complex **1a** (Scheme 1) bearing a phenylethynyl substituent at one β position of each benzopyrrole subunit has recently been identified as one of our best phthalocyanine-based candidate, especially when its intrinsic 2PA cross section ($\sigma_2 = 1010 \text{ GM at } 840 \text{ nm}$) is scaled by the molecular weight.^[21]

Improving the hydrophilicity and the biocompatibility of the known **1a**^[21] or those of its metal-free analogue **2a** (Scheme 1) by replacing the butyl chains on the 2-fluorenyl units by water-solubilizing triethyleneglycol (TEG) chains would allow evaluating the real potential of such systems for photodynamic therapy and fluorescence imaging.

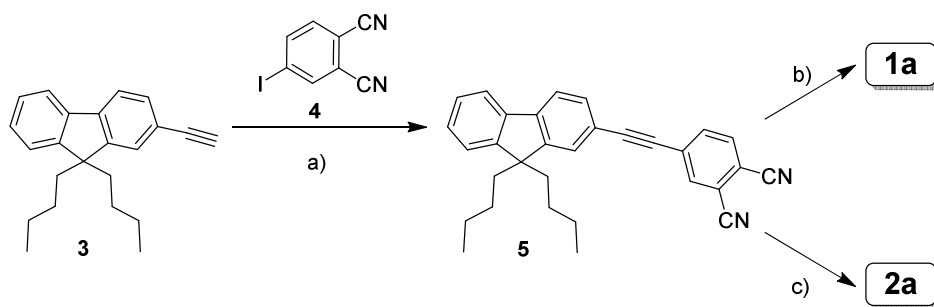


Scheme 1. Hydrophobic fluorenylphthalocyanines and their analogues bearing water-solubilizing groups.

Results and discussion

Synthesis

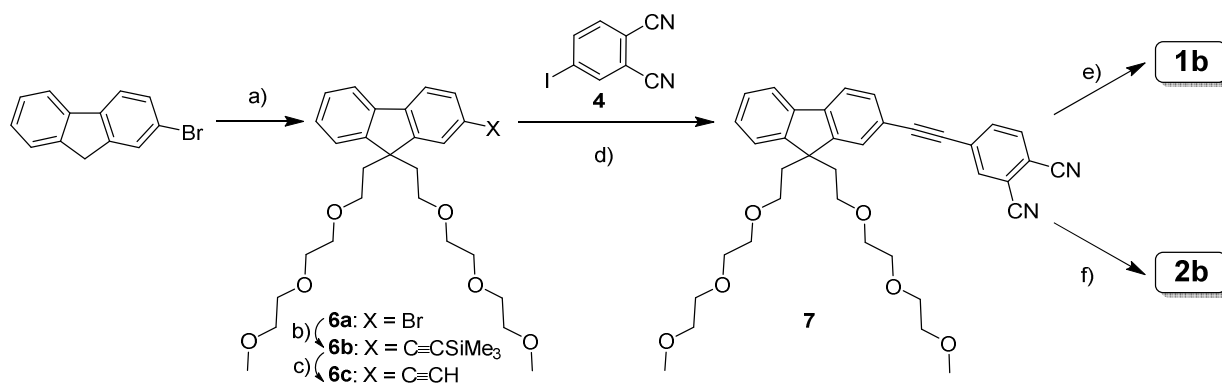
The synthesis of lipophilic zinc phthalocyanine **1a** has been described recently^[21] The corresponding free-base phthalocyanine **2a** was obtained from phthalonitrile **5** by cyclotetramerization in the presence of DBU using *n*-pentanol as high boiling point solvent (Scheme 2). The phthalonitrile **5** was itself obtained from the Sonogashira coupling between 2-ethynylfluorene **3** and iodo derivative **4**.^[21]



Scheme 2. Reagents and conditions: a) Pd(PPh₃)₂Cl₂, CuI, NEt₃/THF, 20 °C, 16h (78%); b) Zn(OAc)₂, DBU/*n*-pentanol, 160 °C, 24h (29%); c) DBU/*n*-pentanol, 160 °C, 16h (24%).

The analogous zinc(II) complex **1b** and free-base phthalocyanine **2b** bearing water-solubilizing chains were synthesized in a similar way from TEG-ylated analogue of **3** (**6c**; Scheme 3). Dialkylation of 2-bromofluorene using 2-[2-(2-methoxyethoxy)ethoxy]ethyl-4-toluenesulfonate in presence of sodium hydroxide and tetrabutylammonium bromide gave **6a**. The Sonogashira coupling of **6a** with trimethylsilylacetylene afforded **6b**, which was deprotected with K₂CO₃ in a mixture of methanol, dichloromethane and THF to afford ethynylfluorene **6c**. The Sonogashira coupling of **6c** with 3-iodophthalonitrile **4** afforded fluorenylphthalonitrile **7**, which was cyclotetramerized in the presence and in the absence of zinc acetate to afford **1b** and **2b**, respectively.

Compounds **1a-b** and **2a-b** were obtained as mixtures of positional isomers, as it is usually the case for tetrasubstituted phthalocyanines, and were characterized by usual techniques, including HRMS and elemental analysis. ¹H and ¹³C NMR spectra were recorded in THF-*d*₈, solvent in which these compounds exhibit good solubilities. The zinc(II) complexes **1a-b** appeared to be essentially non-aggregated in this solvent, but some tendency to aggregate can be deduced from the peak broadening in the ¹H NMR spectra of metal-free phthalocyanines **2a-b**.



Scheme 3. Reagents and conditions: a) $\text{CH}_3(\text{OCH}_2)_3\text{OTs}$, Bu_4NBr , NaOH , toluene, 80°C , 15h (87%); b) ethynyltrimethylsilane, $\text{Pd}(\text{PPh}_3)_2\text{Cl}_2$, CuI , $i\text{Pr}_2\text{NH}/\text{DMF}$, 95°C , 48h (53%); c) K_2CO_3 , $\text{CH}_2\text{Cl}_2/\text{MeOH}/\text{THF}$, 40°C , overnight (99%); d) $\text{Pd}(\text{PPh}_3)_2\text{Cl}_2$, CuI , NEt_3/THF , 20°C , 16h (73%); e) $\text{Zn}(\text{OAc})_2$, $\text{DBU}/n\text{-pentanol}$, 160°C , 24h (18%); f) $\text{DBU}/n\text{-pentanol}$, 160°C , 16h (9%).

Photophysical properties

The relevant photophysical characteristics of the fluorenyl phthalocyanines **1a-b** and **2a-b** are gathered in Table 1, using the unsubstituted zinc phthalocyanine (ZnPc) as a reference.

Absorption spectra have been measured in THF (Figure 1) because all hydrophobic and hydrophilic compounds are soluble in this solvent.¹ At the low concentration used for UV-visible measurements ($\sim 5 \times 10^{-6}$ M), they do not show any sign of aggregation (except perhaps for **2b**, whose absorption spectrum seems slightly broadened in comparison with its analog **2a**). The zinc(II) complexes **1a-b**, which differ only by the R substituents on their fluorenyl units, exhibit exactly the same absorption spectra. These spectra are similar to that of ZnPc , which feature a strong and narrow Q-band in the red region of the visible, and a broader and less intense B-band in the near-UV. However, in comparison with ZnPc , the Q-

¹ These compounds do not fluoresce in water-dimethylsulfoxide [99:1] mixtures ($\Phi_F \approx 0$) and appear extremely aggregated in such media; as indicated by their UV spectra (Figure S6).

bands of **1a** and **1b** are bathochromically (31 nm) and hyperchromically shifted, and their B-bands are hidden by another more intense and broader absorption band corresponding to an intra-ligand (IL) transition of the fluorenyl arms. As expected, the Q-band of free-bases **2a** and **2b** is split into two bands near 700 nm, whereas their fluorenyl-centered band is very similar to that of **1a-b**, and no shift is observed for any band, meaning that replacing butyl chains with triethyleneglycol chains has a very limited effect on the absorption properties of these metal-free compounds (Figure 1).

Compounds **1a-b** and **2a-b** exhibit a strong red emission, characteristic of their phthalocyanine core, with a red-shift of 35 nm for the zinc complexes **1a-b** and of 55 nm for the metal-free phthalocyanines **2a-b**, in comparison with the emission maximum of unsubstituted ZnPc (Table 1 and Figure 2, top). The chain replacement on the fluorenyl units seems to have also a very limited influence, if any, on the emission spectra. Upon excitation at the fluorenyl band in the UV range, no residual emission from these arms was observed in the violet-blue range, but only the typical red emission from the macrocycle, with almost the same quantum yields than those obtained upon excitation at the Q band (Figure 2, bottom). This means that an efficient energy transfer (TBET) process occurs from the peripheral fluorenyl arms toward the phthalocyanine core for all compounds **1a-b** and **2a-b**.

The fluorescence quantum yields of the fluorenylphthalocyanines are higher than that of ZnPc, the highest values being obtained, without surprise, with the metal-free compounds **2a-b**. The replacement of the butyl by TEG chains has apparently a very limited influence on the fluorescence quantum yields.

The properties of oxygen photosensitization were determined by measuring the phosphorescence of singlet oxygen at 1270 nm in a 99:1 mixture of toluene/pyridine (THF could not be used for these measurements, because oxygen is almost non emissive^[22] in this solvent). The zinc(II) phthalocyanines **1a** and **1b** exhibit singlet oxygen quantum yields (0.60

and 0.57, respectively) quite similar to that of ZnPc (0.61), but these measurements could not be done for metal-free phthalocyanines **2a-b** due to their insolubility in toluene/pyridine (99:1).

Table 1. Photophysical properties of phthalocyanines ZnPc, **1a-b** and **2a-b** in THF.

Cpd	λ_{abs} (nm)			ϵ_{max} ($\text{M}^{-1} \text{cm}^{-1}$)	λ_{em} (nm)	Φ_{F} ^a	Φ_{Δ} ^b	σ_2^{max} (GM) ^c
	arms	B band	Q band					
ZnPc	-	343	602, 666	234000	671, 741	0.26	0.61	150
1a	338		628, 697	398000	706, 781	0.29	0.60	1010
1b	338		628, 697	371000	705, 780	0.31	0.57	950
2a	340		626, 657, 688, 721	178000	727, 811	0.35	-	890
2b	340		628, 658, 689, 720	133000	726, 810	0.37	-	720

^a Fluorescence quantum yield in THF determined relative to (Py)ZnPc in a toluene/pyridine (99:1) mixture.^[15]

^b Singlet oxygen production quantum yield in a toluene/pyridine (99:1) mixture relative to ZnPc ($\Phi_{\Delta} = 0.61$) in the same mixture.^[14] ^c Intrinsic 2PA cross-sections at 840 nm measured by 2PEF in the femtosecond regime; a fully quadratic dependence of the fluorescence intensity on the excitation power was always observed in the spectral range investigated (840-1000 nm).

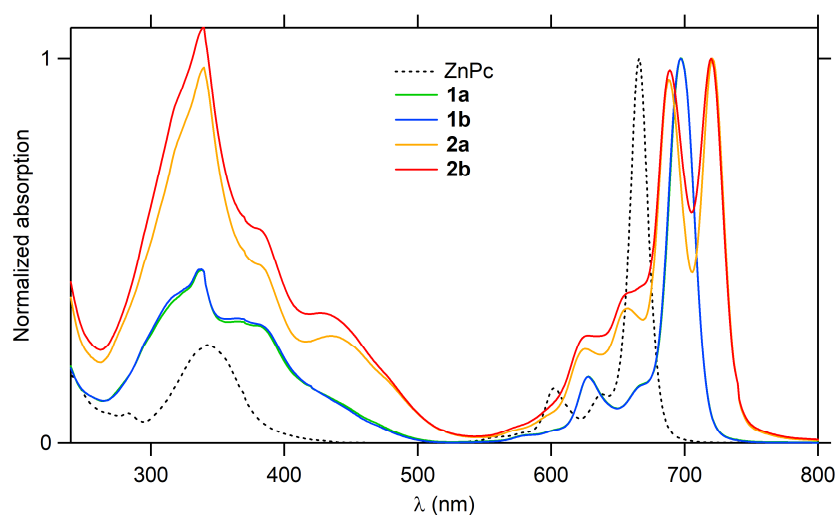


Figure 1. Normalized absorption spectra of ZnPc, **1a-b** and **2a-b** in THF.

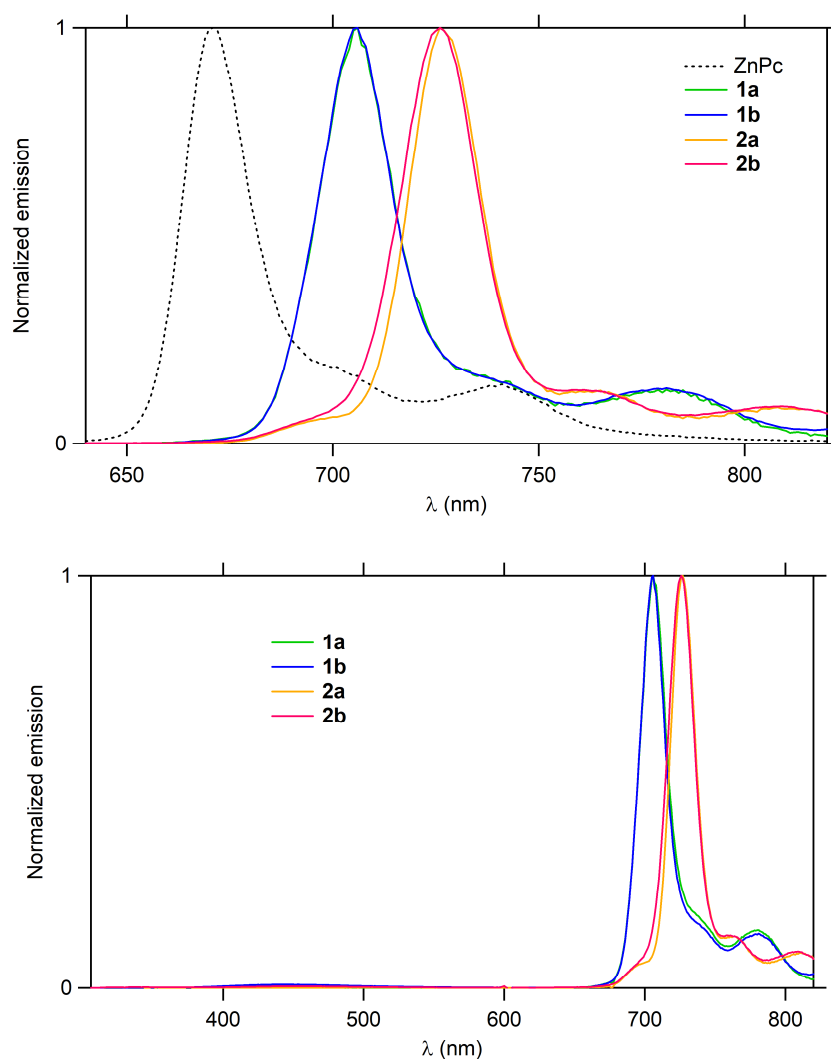


Figure 2. Normalized emission spectra of ZnPc, **1a-b** and **2a-b** in THF upon excitation at the phthalocyanine Q band (top); normalized emission spectra of **1a-b** and **2a-b** in THF after excitation into the fluorenyl band at 300 nm (bottom).

The two-photon absorption cross-sections (σ_2) of the fluorenyl phthalocyanines **1a-b** and **2a-b** in the NIR were then determined by studying in the femtosecond regime their two-photon excited fluorescence (2PEF) properties in THF solution. A fully quadratic dependence of the fluorescence intensity was observed in each case in the 840-1000 nm range, confirming that the measured cross-sections are solely due to 2PA. The highest σ_2 values were obtained at 840 nm (Table 1), but other maxima or shoulders were observed at 890 and 960 nm (Figure 3). A large increase in the first σ_2 maximum relative to that measured for ZnPc (150 GM at 840 nm) was observed for all fluorenyl phthalocyanines in the whole spectral range. Zinc

phthalocyanines **1a-b** exhibit larger σ_2 values (1010 and 950 GM, respectively) than the corresponding metal-free compounds **2a-b** (890 and 720 GM, respectively). The 2PA spectrum of phthalocyanine **1b** (with TEG chains) is very similar to that of its analog **1a** (with butyl chains), and this observation can also be made for **2b** and its analog **2a**. The 2PA cross-sections of the phthalocyanines bearing TEG chains are lower than those of the corresponding compound bearing butyl chains, but this decrease is at the limit of the experimental errors for 2PEF measurements ($\pm 10\%$).

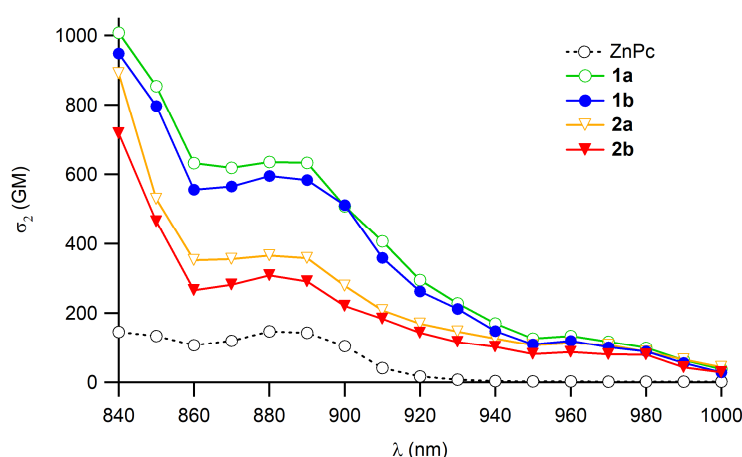


Figure 3. Two-photon absorption spectra of ZnPc, **1a-b** and **2a-b** in THF.

The combination of maintained singlet oxygen quantum yield (Φ_Δ) with slightly increased fluorescence quantum yield and strongly increased 2PA cross sections (σ_2) compared with ZnPc leads also to significant enhancements of the figure of merit traditionally used for gauging the two-photon excited oxygen sensitization ($\sigma_2\Phi_\Delta$) or the two-photon induced fluorescence ($\sigma_2\Phi_F$). In comparison with ZnPc, a ~ 6 -fold enhancement of $\sigma_2\Phi_\Delta$ was obtained at 840 nm for **1a-b**, together with a ~ 7 - to 8-fold enhancement of two-photon brightness ($\sigma_2\Phi_F$) for **1a-b** and **2a-b**.

Biological properties

The potential of **1b** and **2b** for cell imaging and PDT was studied on MCF-7 human breast cancer cells under both 1-photon excitation (1PE) and 2-photon excitation (2PE). Their biocompatibility was first determined *in vitro*. To do so, MCF-7 cells were incubated in the dark for 72 h, in presence of increasing concentrations of phthalocyanines (from 0.1 to 200 $\mu\text{g mL}^{-1}$). No cytotoxicity was evidenced for **1b** up to 25 $\mu\text{g mL}^{-1}$, but **1a** was slightly more cytotoxic with a 20% cell death at 25 $\mu\text{g mL}^{-1}$ and 30% cell death at 50 $\mu\text{g mL}^{-1}$ (Figure 4). More significant cytotoxicity was observed in the absence of light for both compounds for concentrations higher than 50 $\mu\text{g mL}^{-1}$, up to 60 % and 50% cell death for **1a** and **1b**, respectively, at a concentration of 200 $\mu\text{g mL}^{-1}$.

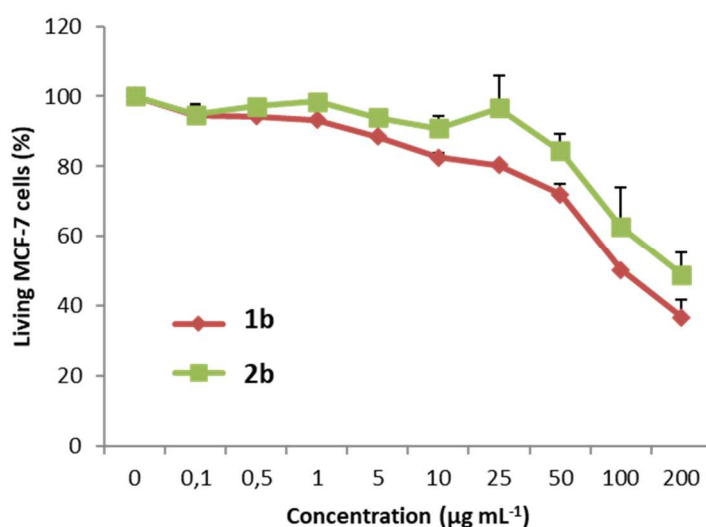


Figure 4. Biocompatibility analysis. Dark cytotoxicity study of MCF-7 human breast cancer cells incubated for 72 h with phthalocyanines at a range from 0.1 to 200 $\mu\text{g mL}^{-1}$. The percentage of living cells was measured by a MTT assay performed at the end of the incubation time. Values are means \pm standard deviations of 3 experiments.

The efficiency of these photosensitizers for one-photon excited photodynamic therapy (1P-PDT) was subsequently studied. MCF-7 cells were incubated during 16 h with these phthalocyanines at a concentration of 25 $\mu\text{g mL}^{-1}$ and then irradiated for 10 min (or not) with the mercury lamp of a standard fluorescence microscope ($\lambda_{\text{exc}} = 390\text{-}420\text{ nm}$, 39 J cm^{-2}). The cell death quantification assay (MTT) performed two days after the irradiation demonstrated a decrease in living cells with both compounds. Data reported in Figure 5A show that irradiation alone is not cytotoxic. Likewise, metal-free phthalocyanine **2b** is not cytotoxic without irradiation, but significant dark cytotoxicity is observed with zinc complex **1b**, in agreement with data of Figure 4. The 1P-PDT efficacy of both compounds was demonstrated by the difference between irradiated and non-irradiated conditions of 44% and 34% of cell death for **1b** and **2b**, respectively, the highest cell death level being observed for **1b** with only 17% of living cells after treatment and irradiation (Figure 5A).

Since the PDT is a mechanism connected with an intracellular increase in reactive oxygen species (ROS), the ROS production during 1PE-PDT experiments was subsequently investigated. Thus, cells were treated with the phthalocyanines under the same conditions as those used for PDT, but were incubated at 37 °C with 20 μM H₂DCFDA (2',7'-dichlorodihydrofluorescein diacetate) 45 min before irradiation. After irradiation for 10 min ($\lambda_{\text{exc}} = 390\text{-}420\text{ nm}$, 39 J cm^{-2}), cells were rinsed twice with cell media and the fluorescence of 2',7'-dichlorofluorescein (DCF) was collected using the camera of a standard fluorescence microscope. The generation of ROS during the PDT experiment (Figure 5B, top) is indicated by the green luminescence of DCF at 535 nm. The lower quantity of live cells with **1b** than with **2b** after rinsing and removal of senescent cells is probably due to the higher cytotoxicity of **1b**. In the absence of irradiation (control), no luminescence was detected (Figure 5B, bottom).

The one-photon imaging potential of **1b** and **2b** was also studied. For this, MCF-7 cells were incubated for 16 h with the phthalocyanines at a concentration of 25 $\mu\text{g mL}^{-1}$. Fluorescence

imaging was performed at $\lambda_{\text{exc}} = 390\text{-}420$ nm with the mercury lamp of a standard microscope and magnification 40 \times . In these conditions, **1b** is clearly much brighter than **2b** (Figure 5C).

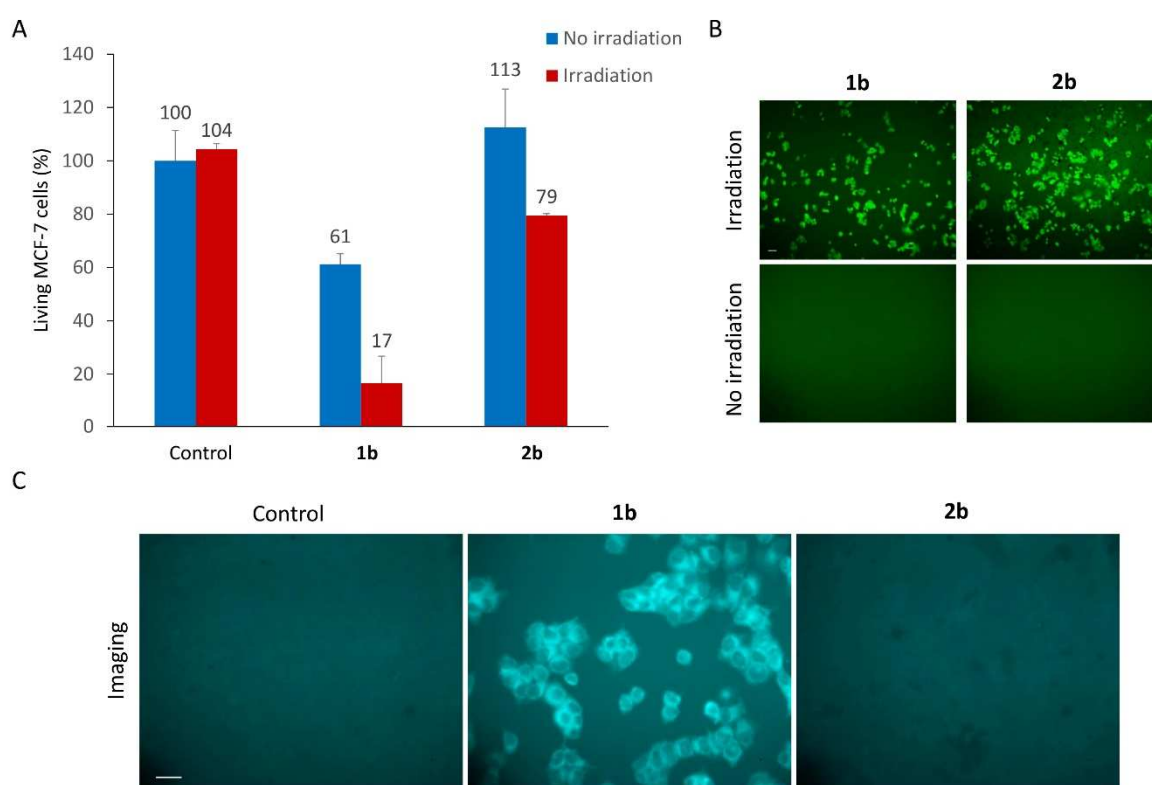


Figure 5. One-photon PDT, ROS production and fluorescence imaging of phthalocyanines on cancer cells. Living MCF-7 breast cancer cells were incubated with **1b** and **2b** for 16 h at a concentration of $25 \mu\text{g mL}^{-1}$. **(A)** PDT experiment was performed at $\lambda_{\text{exc}} = 390\text{-}420$ nm, with 10 min irradiation time (magnification 10 \times). Two days after excitation, MTT assay was performed to quantify living cells. Values are the mean of 2 independent experiments performed in triplicate and error bars represent the standard deviation. **(B)** Analysis of ROS production during irradiation (same conditions as PDT experiment) of cells incubated with phthalocyanines. **(C)** Fluorescence imaging was performed at $\lambda_{\text{exc}} = 390\text{-}420$ nm and magnification 40 \times (Scale bar: 10 μm).

Finally, the efficacy of these compounds in 2PEF imaging and two-photon PDT was also investigated. Living MCF-7 breast cancer cells were thus incubated for 16 h with phthalocyanines at a concentration of $25 \mu\text{g mL}^{-1}$. Figure 6A shows that both compounds are efficiently internalized and highly luminescent upon excitation in the NIR at 840 nm with a confocal microscope (LSM 780, Chameleon femtosecond laser). The localization of **1b** and **2b** is clearly inside the cells, as confirmed by the repartition of compounds all around the nucleus (black circles) in all the cytoplasm (ESI; Figure S7). Then, to determine their 2PE-PDT efficacy, MCF-7 cells were irradiated at 840 nm by 3 scans of 1.57 sec each, with a focused laser beam at the maximum laser power (Figure 6B). Metal-free phthalocyanine **2b** exhibits no significant cytotoxicity without irradiation (in agreement with data of Figures 4 and 5A), whereas upon irradiation of less than 5 seconds ($3 \times 1.57 \text{ sec}$), a decrease of living cells of $\sim 50\%$ was observed. An even stronger efficacy was obtained upon irradiation with zinc phthalocyanine **1b** (77% cell death), but along with a high dark cytotoxicity (63% cell death).²

² A discrepancy between the dark toxicity values obtained during the 1PE and the 2PE experiments can be noticed in the case of **1b**, which can be explained by differences in the experimental protocols. In particular, when a compound exhibiting some dark toxicity is used, the glass bottom of the 384-well plates used for 2PE experiments often leads to an increase of the dark cell death, whereas cells are usually more resistive with the plastic bottom of the 96-well plates used for 1PE experiments.

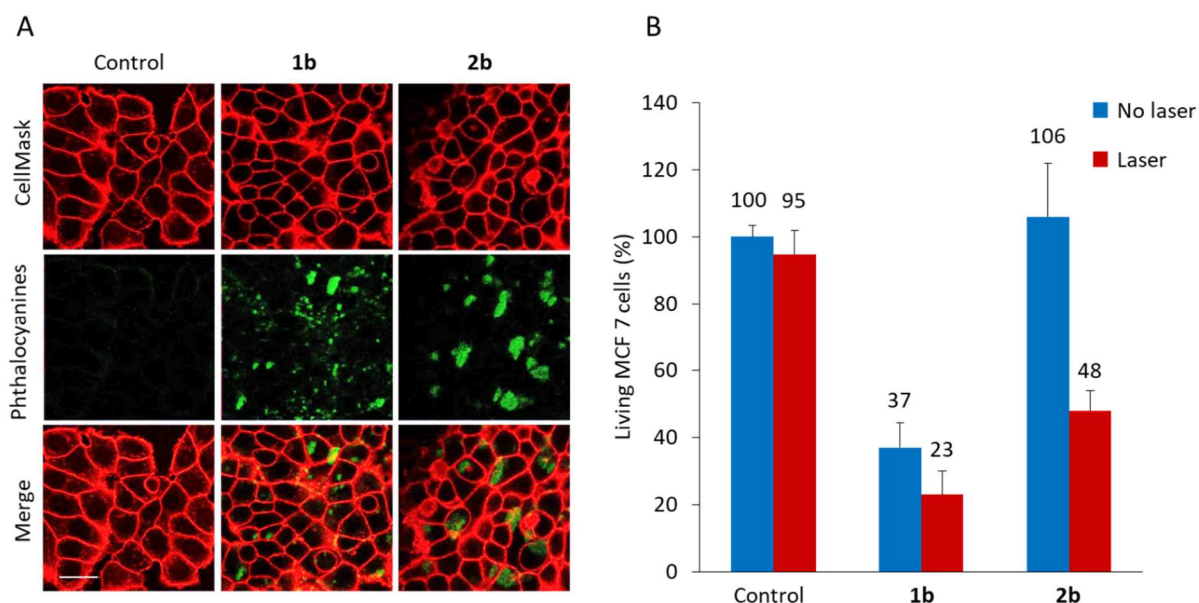


Figure 6. Two-photon imaging and PDT potential of phthalocyanines on cancer cells.

Living MCF-7 breast cancer cells were incubated for 16 h with **1b** and **2b** at a concentration of $25 \mu\text{g mL}^{-1}$. **(A)** Two-photon excited fluorescence imaging was performed with LSM780 confocal microscope (Chameleon femtosecond laser), $\lambda_{\text{exc}} = 840 \text{ nm}$ and magnification $63\times$. Cell membranes were stained with CellMask Orange (in red, $\lambda_{\text{exc}} = 561 \text{ nm}$) and phthalocyanines appear in green. **(B)** 2P-PDT was performed with the same microscope, $\lambda_{\text{exc}} = 840 \text{ nm}$, (laser input 3W) and magnification $10\times$ (Scale bar: $10 \mu\text{m}$). Cells were irradiated by 3 pulses of 1.57 s each. Two days after excitation, MTT assay was performed to quantify living cells. Values are the mean of 2 independent experiments performed in triplicate and error bars represent the standard deviation.

To conclude, fluorenylphthalocyanines **1b** and **2b** bearing water-solubilizing (TEG) groups exhibit photophysical properties (1PA and 2PA, fluorescence and singlet oxygen quantum yields) similar to those of their lipophilic analogues **1a** and **2a**. Accordingly, 6 to 8-fold enhancements of their two-photon brightness and oxygen photosensitization are obtained relative to ZnPc, motivating studies of their imaging and PDT potential. Preliminary *in vitro*

experiments were thus conducted on human breast cancer cells. Biocompatibility studies showed that metal-free phthalocyanine **2b** is non-toxic in the dark, which is less the case of its zinc complex analogue **1b**. Under one-photon excitation, **1b** exhibits a higher potential for both PDT and imaging than **2b**, but in contrast under two-photon excitation in the NIR, **2b** is more promising than **1b** for PDT, whereas the two compounds exhibit similar brightness, allowing to monitor their distribution and their internalization within cells.

These compounds, especially metal-free **2b**, are thus efficient for combined one- and two-photon PDT and fluorescence imaging, demonstrating a real theranostic potential.

Experimental Section

Details of the spectroscopic measurements,^[20g] of singlet oxygen quantum yields measurements (Φ_{Δ})^[19j] or of two-photon absorption experiments^[20f] have been previously described and will only be briefly recalled in the ESI. General synthetic methods as well as procedures and characterization data for intermediate compounds **5** and **6a-c** can also be found in the ESI.

Synthetic procedures

4-((9,9-Bis(2-(2-(2-methoxyethoxy)ethoxy)ethyl)-9H-fluoren-2-yl)ethynyl)phthalonitrile (7). In a Schlenk tube, a mixture of alkyne **6c** (362 mg, 0.75 mmol, 1.5 eq), 4-iodophthalonitrile (127 mg, 0.5 mmol, 1 eq), Pd(PPh₃)₂Cl₂ (3.5 mg, 0.005 mmol, 1% eq) and CuI (0.6 mg, 0.003 mmol, 0.6% eq) in THF (2 mL) and NEt₃ (8 mL) was stirred for 16 hours at room temperature under argon atmosphere. After evaporation of the solvents, the residue was filtered and extracted three times with CH₂Cl₂. The organic layer was dried with MgSO₄, filtered and the solvent was evaporated. The crude product was purified by chromatography

(CH₂Cl₂/MeOH [50:1]), to give **7** as a yellow oil (222 mg, 73% yield). ¹H NMR (400 MHz, CDCl₃): δ 7.95 (s, 1H), 7.85 (dd, *J*₁ = 8.1, *J*₂ = 1.6 Hz, 1H), 7.80 (d, *J* = 8.3 Hz, 1H), 7.72 – 7.66 (m, 2H), 7.61 (s, 1H), 7.53 (dd, *J*₁ = 7.8, *J*₂ = 1.5 Hz, 1H), 7.46 – 7.41 (m, 1H), 7.39 – 7.32 (m, 2H), 3.52 – 3.44 (m, 8H), 3.40 – 3.35 (m, 4H), 3.32 (s, 6H), 3.23 – 3.16 (m, 4H), 2.81 – 2.70 (m, 4H), 2.45 – 2.34 (m, 4H). ¹³C NMR (101 MHz, CDCl₃): δ 149.4, 149.3, 142.3, 139.3, 135.9, 135.5, 133.5, 131.5, 129.5, 128.4, 127.6, 126.9, 123.3, 120.5, 120.0, 119.7, 116.3, 115.3, 114.8, 114.1, 97.7, 86.3, 71.9, 70.4, 70.0, 66.9, 59.0, 51.4, 39.6. FT-IR ν (cm⁻¹): 3067 (w, Ar-H), 2920-2817 (s, Aliph. C-H), 2234 (m, C≡N), 2203 (s, C≡C), 1593, 1546, 1494, 1452, 1419, 1246, 1199, 1100, 1026, 1026, 910, 842, 739. HRMS-ASAP: *m/z* = 602.2883 [M]⁺ (calcd for C₃₇H₄₀N₂O₆: 602.28809).

Zinc phthalocyanine 1a. A mixture of phthalonitrile **5** (200 mg, 0.47 mmol, 1 eq), anhydrous Zn(OAc)₂ (42 mg, 0.23 mmol, 0.5 eq) and 1,8-diazabicyclo[5.4.0]undec-7-ene (DBU) (5 drops) in degassed *n*-pentanol (2 mL) was heated at 160 °C for 24 h under argon. The green solution was cooled to room temperature and the suspension was poured into cold methanol. The dark green precipitate was then filtered off and washed with hot methanol. The crude product was purified by column chromatography on silica gel (CH₂Cl₂/heptane [1:1]) and finally recrystallized from MeOH/CH₂Cl₂. The zinc complex **1a** was obtained as a green solid (61 mg, 29% yield). ¹H NMR (400 MHz, THF-*d*₈): δ 9.36 – 9.19 (m, 4H), 9.15 – 8.99 (m, 4H), 8.33 – 8.19 (m, 4H), 7.97 (s, 4H), 7.91 – 7.75 (m, 12H), 7.56 – 7.46 (m, 4H), 7.44 – 7.34 (m, 8H), 2.37 – 2.15 (m, 16H), 1.32 – 1.20 (m, 16H), 0.92 – 0.70 (m, 40H). ¹³C NMR (101 MHz, THF-*d*₈): δ 151.2, 151.1, 142.5, 140.8, 134.0, 131.1, 127.9, 127.2, 126.3, 125.1, 125.0, 124.5, 124.1, 123.1, 121.5, 121.4, 120.4, 120.0, 92.3, 88.0, 55.3, 40.4, 26.3, 23.3, 13.6. FT-IR (cm⁻¹): $\bar{\nu}$ = 3063 (w, Ar-H), 2956-2861 (s, Aliph. C-H), 2198 (w, C≡C), 1608, 1491, 1465, 1450, 1392, 1334, 1298, 1261, 1143, 1087, 1047, 940, 892, 828, 775, 735. HRMS-ESI: *m/z* 1776.8274 [M]⁺ (calcd for C₁₂₄H₁₁₂N₈Zn: 1776.8295). Anal. Calcd. (%) for

C₁₂₄H₁₁₂N₈Zn•2CH₃OH: C, 82.13; H, 6.68; N, 5.99. Found: C, 81.93; H, 6.40; N, 6.21.

Zinc phthalocyanine 1b. A mixture of phthalonitrile **7** (200 mg, 0.33 mmol, 1 eq), anhydrous Zn(OAc)₂ (30 mg, 0.16 mmol, 0.5 eq) and 1,8-diazabicyclo[5.4.0]undec-7-ene (DBU) (5 drops) in degassed *n*-pentanol (2 mL) was heated at 160 °C for 24 h under argon. The green solution was cooled to room temperature and the solvent was evaporated. The residue was extracted three times with CH₂Cl₂. The organic layer was dried with MgSO₄, filtered and the solvent was evaporated. The crude product was purified by column chromatography on silica gel (CH₂Cl₂/EtOH [20:1]), affording the zinc complex **1b** as a green oil (37 mg, 18% yield). ¹H NMR (400 MHz, THF-*d*₈) δ 9.32 – 9.20 (m, 4H), 9.17 – 9.03 (m, 4H), 8.33 – 8.25 (m, 4H), 8.09 (s, 4H), 7.96 – 7.78 (m, 12H), 7.69 – 7.62 (m, 4H), 7.50 – 7.37 (m, 8H), 3.60 – 3.49 (m, 16H), 3.49 – 3.40 (m, 32H), 3.34 – 3.23 (m, 40H), 3.20 – 2.90 (m, 16H), 2.69 – 2.48 (m, 16H). ¹³C NMR (101 MHz, THF-*d*₈) δ 152.7, 150.4, 141.5, 140.4, 138.5, 137.5, 132.3, 131.7, 128.1, 127.6, 127.1, 125.9, 125.8, 124.9, 123.8, 122.9, 122.7, 120.7, 120.4, 92.8, 91.3, 72.3, 70.8, 70.5, 67.5, 58.4, 52.0, 40.0. FT-IR (cm⁻¹): $\bar{\nu}$ = 3059 (w, Ar-H), 2917-2813 (s, Aliph. C-H), 2197 (vw, C≡C), 1608, 1491, 1465, 1450, 1387, 1299, 1248, 1198, 1090, 1046, 943, 889, 831, 777, 727. HRMS-ESI: *m/z* 2497.0811 [M]⁺ (calcd for C₁₄₈H₁₆₀N₈O₂₄Zn: 2497.0832). Anal. Calcd. (%) for C₁₄₈H₁₆₀N₈O₂₄Zn•CH₂Cl₂: C, 69.22; H, 6.32; N, 4.33. Found: C, 69.47; H, 6.32; N, 4.36.

Metal-free phthalocyanine 2a. A mixture of phthalonitrile **5** (200 mg, 0.47 mmol) and 1,8-diazabicyclo[5.4.0]undec-7-ene (DBU) (5 drops) in degassed *n*-pentanol (2 mL) was heated at 160 °C and stirred for 16 h under argon. The solution was allowed to cool to room temperature and poured into cold methanol, left for 0.5 h and the crude product was filtered off. Then, this solid was washed with water and hot methanol, and dried under vacuum. The green product was filtered through a pad of silica (heptane/CH₂Cl₂ 2:1) and then

recrystallized from MeOH/CH₂Cl₂. Metal-free phthalocyanine **2a** was obtained as a green solid (48 mg, 24% yield). ¹H NMR (400 MHz, THF-*d*₈) δ 8.95 – 8.14 (m, 8H), 8.10 – 7.61 (m, 20H), 7.58 – 7.31 (m, 12H), 2.43 – 2.11 (m, 16H), 1.37 – 1.15 (m, 16H), 0.98 – 0.66 (m, 40H). ¹³C NMR (101 MHz, THF-*d*₈) δ 151.3, 151.0, 142.0, 141.9, 141.0, 131.7, 127.9, 127.2, 126.3, 123.1, 122.4, 120.5, 120.2, 93.0, 90.7, 55.5, 40.6, 26.5, 23.5, 13.9. FT-IR (cm⁻¹): $\bar{\nu}$ = 3290 (w, N-H), 3063 (w, Ar-H), 2956-2857 (s, Aliph. C-H), 2198 (w, C≡C), 1612, 1488, 1450, 1415, 1378, 1297, 1264, 1140, 1091, 1007, 930, 893, 829, 737, 717. HRMS-ESI: *m/z* 1714.9149 [M]⁺ (calcd for C₁₂₄H₁₁₄N₈: 1714.9161). Anal. Calcd. (%) for C₁₂₄H₁₁₄N₈•3C₇H₁₆: C, 86.36; H, 7.96; N, 5.67. Found: C, 86.17; H, 7.60; N, 5.23.

Metal-free phthalocyanine 2b. A mixture of phthalonitrile **7** (200 mg, 0.33 mmol) and 1,8-diazabicyclo[5.4.0]undec-7-ene (DBU) (5 drops) in degassed *n*-pentanol (2 mL) was heated to 160 °C and stirred for 16 h under argon. The solution was allowed to cool to room temperature and poured into cold methanol, left for 0.5 h and the crude product was filtered off. Then, this solid was washed with water and hot methanol, and dried under vacuum. The green product was filtered through a pad of silica (heptane/CH₂Cl₂ [2:1]). Metal-free phthalocyanine **2b** was obtained as a green oil (18 mg, 9% yield). ¹H NMR (400 MHz, THF-*d*₈) δ 9.04 – 8.64 (m, 8H), 8.26 – 8.05 (m, 8H), 7.98 – 7.75 (m, 12H), 7.72 – 7.62 (m, 4H), 7.52 – 7.38 (m, 8H), 3.61 – 3.52 (m, 16H), 3.51 – 3.41 (m, 32H), 3.41 – 3.19 (m, 40H), 3.16 – 2.92 (m, 16H), 2.72 – 2.51 (m, 16H), -3.68 (s, 2H). ¹³C NMR (101 MHz, THF-*d*₈) δ = 150.5, 141.6, 140.4, 132.8, 132.0, 128.1, 127.7, 127.1, 125.4, 123.9, 122.5, 120.8, 120.6, 93.5, 91.1, 72.3, 70.8, 70.5, 67.6, 58.4, 52.1, 40.0. FT-IR (cm⁻¹): $\bar{\nu}$ = 3288 (w, N-H), 3063 (w, Ar-H), 2921-2813 (s, Aliph. C-H), 2200 (vw, C≡C), 1614, 1493, 1465, 1451, 1352, 1300, 1260, 1199, 1098, 1014, 940, 889, 831, 763, 746. HRMS-ESI: *m/z* 2435.1711 [M]⁺ (calcd for C₁₄₈H₁₆₂N₈O₂₄: 2435.1697). Anal. Calcd. (%) for C₁₄₈H₁₆₂N₈O₂₄•CH₂Cl₂: C, 70.96; H, 6.55; N, 4.44. Found: C, 70.79; H, 6.40; N, 4.28.

Cell culture. MCF-7 human breast cancer cells (purchased from ATCC) were cultured in DMEM F12 Media - GlutaMAX™-I (containing 4.5 g.L⁻¹ of D-glucose) supplemented with 10% fetal bovine serum, 1% penicillin/streptomycin and allowed to grow in humidified atmosphere at 37 °C under 5 % CO₂.

Cytotoxicity study. MCF-7 cells were seeded into 96-well plates at 2000 cells per well in 200 μL culture medium and allowed to grow for 24 h. Increasing concentrations of phthalocyanines were added to the culture medium of MCF-7 cells, and after 3 days a MTT assay was performed to determine the cell viability. Briefly, cells were incubated for 4 h with 0.5 mg mL⁻¹ of MTT (3-(4,5-dimethylthiazol-2-yl)-2,5-diphenyltetrazolium bromide; Promega) in media. The MTT/media solution was then removed and the precipitated crystals were dissolved in EtOH/DMSO (v/v). The solution absorbance was read at 540 nm in a microplate reader.

One-photon photodynamic therapy. MCF-7 cancer cells were seeded into 96-well plates at a concentration of 1000 cells per well in 100 μL of culture medium and allowed to grow for 24 h. Then, cells were incubated for 24 h, with or without 25 μg mL⁻¹ addition of phthalocyanines. After incubation, cells were irradiated for 10 min or not with the mercury lamp of a standard fluorescence microscope ($\lambda_{exc} = 390-420$ nm, 39 J cm⁻²). Two days after irradiation, MTT assay was performed to measure the level of living cells.

ROS imaging under 1PE. The detection of intracellular reactive oxygen production (ROS) was performed using DCF-DA Cellular ROS Detection Assay Kit (abcam). For this, cells were seeded into 96-well plates at a concentration of 1000 cells per well in 100 μL of culture

medium and allowed to grow for 24 h. Then, cells were incubated 16 h with or without 25 $\mu\text{g mL}^{-1}$ of phthalocyanines. The detection of ROS production is performed during a phototoxicity experiment for which, 45 min before irradiation, cells were incubated at 37°C with 20 μM of H₂DCF-DA (abcam). After irradiation for 10 min ($\lambda_{\text{exc}} = 390/420 \text{ nm}$, 39 J cm⁻²), cells were rinsed twice with cell media and the fluorescence emission of DCF ($\lambda_{\text{exc}} = 450 \text{ nm}$) was collected using the camera of a standard fluorescence microscope. The green luminescence of DCF detected at 535 nm traduces the generation of ROS.

Two-photon fluorescence imaging. Cells were seeded onto bottom glass dishes (World Precision Instrument, Stevenage, UK) at a density of 10⁶ cells cm⁻² in culture medium during 24 h. Then, the cells were incubated overnight with the phthalocyanines at a concentration of 25 $\mu\text{g mL}^{-1}$. For cell membrane staining, 15 minutes before the end of incubation, cells were loaded with CellMask Orange (Invitrogen, Cergy Pontoise, France) at a final concentration of 5 $\mu\text{g mL}^{-1}$. Before imaging, cells were washed twice with culture medium. Fluorescence imaging was performed on living cells with a LSM 780 LIVE confocal microscope (Carl Zeiss, Le Pecq, France), at 840 nm for phthalocyanines and 561 nm for CellMask Orange. All images were performed with a high magnification (63×/1.4 OIL DIC Plan-Apo).

Two-photon photodynamic therapy. Cells were seeded into 384-well glass bottomed plate (thickness 0.17 mm) with a black polystyrene frame, at 500 cells per well in 50 μL of culture medium and allowed to grow for 24 h. Then, cells were incubated for 24 h with phthalocyanines at a concentration of 25 $\mu\text{g mL}^{-1}$. After incubation, cells were submitted or not to a femtosecond pulsed laser (Chameleon Ultra II, Coherent, generating 140 fs wide pulses at 80 MHz repetition rate). Irradiation was performed on living cells with a LSM 780 LIVE confocal microscope (Carl Zeiss, Le Pecq, France), at 840 nm (10×/0.3) with a focused laser beam and a maximum laser power (3 W input, 900 mW cm⁻² output before the

objective). Half of the well was irradiated at 840 nm by 3 scans of 1.57 s duration in 4 different areas of the well. The scan size does not allow irradiating more areas without overlapping. Two days after irradiation, a MTT assay was performed to determine cell viability. Briefly, cells were incubated for 4 h in the presence of 3-(4,5-dimethylthiazol-2-yl)-2,5-diphenyltetrazolium bromide (MTT, Promega, 0.5 mg mL⁻¹) to determine the mitochondrial enzyme activity. Then, supernatant was removed, and 50 µL of EtOH/DMSO (1:1) was added to dissolve the MTT precipitates. Absorbance was measured at 540 nm with a microplate reader. The value obtained was corrected according to the following formula: Abs “no laser” – 2 × (Abs “no laser” – Abs “laser”).

Acknowledgments

CNRS is acknowledged for its financial support and the “Ministère de l’Enseignement Supérieur et de la Recherche Scientifique de Tunisie” for PhD funding (SA). This project was supported by the departmental committees CD35, CD28 and CD29 of the “*Ligue contre le Cancer du Grand-Ouest*”. Guillaume Clermont (ISM) is also thanked for his help in the two-photon excited fluorescence study and in the singlet oxygen measurements. We acknowledge the imaging facility “Montpellier Ressources Imagerie” (MRI), member of the national infrastructure France-BioImaging supported by the French National Research Agency (ANR-10-INBS-04, «Investments for the future»).

Declaration of competing interest

There are no conflicts to declare.

References

- [1] a) J. P. Celli, B. Q. Spring, I. Rizvi, C. L. Evans, K. S. Samkoe, S. Verma, B. W. Pogue, T. Hasan, *Chem. Rev.* **2010**, *110*, 2795-2838; b) J. F. Lovell, T. W. B. Liu, J. Chen, G. Zheng, *Chem. Rev.* **2010**, *110*, 2839-2857.
- [2] N. L. Oleinick, R. L. Morris, I. Belichenko, *Photochem. Photobiol. Sci.* **2002**, *1*, 1-21.
- [3] B. W. Pedersen, T. Breitenbach, R. W. Redmond, P. R. Ogilby, *Free Radical Res.* **2010**, *44*, 1383-1397.
- [4] L. A. Sordillo, S. Pratavieira, Y. Pu, K. Salas-Ramirez, L. Shi, L. Zhang, Y. Budansky, R. R. Alfano, *Proc. SPIE* **2014**, *8940*, 89400V.
- [5] M. Pawlicki, H. A. Collins, R. G. Denning, H. L. Anderson, *Angew. Chem. Int. Ed.* **2009**, *48*, 3244-3266.
- [6] a) F. Bolze, S. Jenni, A. Sour, V. Heitz, *Chem. Commun*, **2017**, *53*, 12857-12877; b) Z. Sun, L.-P. Zhang, F. Wu, Y. Zhao, *Adv. Funct. Mater.* **2017**, *27*, 1704079.
- [7] a) C. B. Nielsen, M. Johnsen, J. Arnbjerg, M. Pittelkow, S. P. McIlroy, P. R. Ogilby, M. Jorgensen, *J. Org. Chem.* **2005**, *70*, 7065-7079; b) P.-H. Lanoë, T. Gallavardin, A. Dupin, O. Maury, P. L. Baldeck, M. Lindgren, C. Monnereau, C. Andraud, *Org. Biomol. Chem.* **2012**, *10*, 6275-6278; c) C. Tang, P. Hu, E. Ma, M. Huang, Q. Zheng, *Dyes Pigm.* **2015**, *117*, 7-15; d) M. Velusamy, J.-Y. Shen, J. T. Lin, Y.-C. Lin, C.-C. Hsieh, C.-H. Lai, C.-W. Lai, M.-L. Ho, Y.-C. Chen, P.-T. Chou, J.-K. Hsiao, *Adv. Funct. Mater.* **2009**, *19*, 2388-2397; e) C. Rouxel, M. Charlot, Y. Mir, C. Frochot, O. Mongin, M. Blanchard-Desce, *New J. Chem.* **2011**, *35*, 1771-1780.
- [8] a) S. C. Boca, M. Four, A. Bonne, B. van der Sanden, S. Astilean, P. L. Baldeck, G. Lemerrier, *Chem. Commun*, **2009**, 4590-4592; b) L. Zeng, S. Kuang, G. Li, C. Jin, L. Ji, H. Chao, *Chem. Commun*, **2017**, *53*, 1977-1980; c) J. Liu, C. Jin, B. Yuan, X. Liu, Y. Chen, L. Ji, H. Chao, *Chem. Commun*, **2017**, *53*, 2052-2055.
- [9] a) X. Shen, L. Li, A. C. Min Chan, N. Gao, S. Q. Yao, Q.-H. Xu, *Adv. Opt. Mater.* **2013**, *1*, 92-99; b) X. Shen, L. Li, H. Wu, S. Q. Yao, Q.-H. Xu, *Nanoscale* **2011**, *3*, 5140-5146; c) X. Shen, S. Li, L. Li, S. Q. Yao, Q.-H. Xu, *Chem. Eur. J.* **2015**, *21*, 2214-2221.
- [10] A. Sourdon, M. Gary-Bobo, M. Maynadier, M. Garcia, J.-P. Majoral, A.-M. Caminade, O. Mongin, M. Blanchard-Desce, *Chem. Eur. J.* **2019**, *25*, 3637-3649.
- [11] a) M. Gary-Bobo, Y. Mir, C. Rouxel, D. Brevet, I. Basile, M. Maynadier, O. Vaillant, O. Mongin, M. Blanchard-Desce, A. Morère, M. Garcia, J.-O. Durand, L. Raehm,

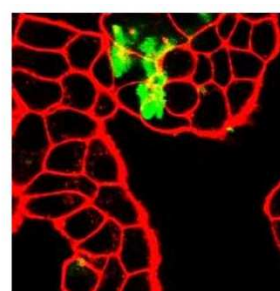
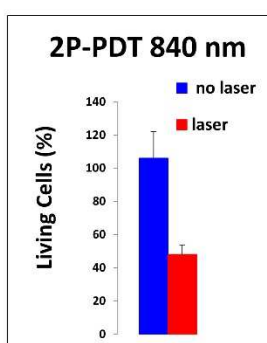
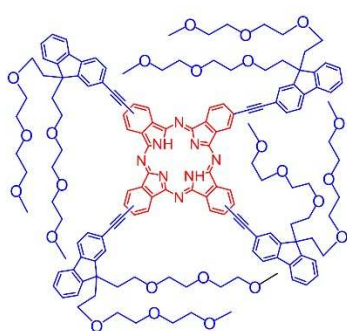
- Angew. Chem. Int. Ed.* **2011**, *50*, 11425-11429; b) O. Vaillant, E. Cheikh Khaled, D. Warther, D. Brevet, M. Maynadier, E. Bouffard, F. Salgues, A. Jeanjean, P. Puche, C. Mazerolles, P. Maillard, O. Mongin, M. Blanchard-Desce, L. Raehm, X. Rébillard, J.-O. Durand, M. Gary-Bobo, A. Morère, M. Garcia, *Angew. Chem. Int. Ed.* **2015**, *54*, 5952-5956.
- [12] S. Singh, A. Aggarwal, N. V. S. D. K. Bhupathiraju, G. Arianna, K. Tiwari, C. M. Drain, *Chem. Rev.* **2015**, *115*, 10261-10306.
- [13] a) L. Roguin, N. Chiarante, M. García Vior, J. Marino, *Int. J. Biochem. Cell Biol.* **2019**, *114*, 105575; b) X. Li, B.-D. Zheng, X.-H. Peng, S.-Z. Li, J.-W. Ying, Y. Zhao, J.-D. Huang, J. Yoon, *Coord. Chem. Rev.* **2019**, *379*, 147-160; c) P.-C. Lo, M. S. Rodríguez-Morgade, R. K. Pandey, D. K. P. Ng, T. Torres, F. Dumoulin, *Chem. Soc. Rev.* **2020**, *49*, 1041-1056.
- [14] a) M. van Leeuwen, A. Beeby, S. H. Ashworth, *Photochem. Photobiol. Sci.* **2010**, *9*, 370-375; b) M. van Leeuwen, A. Beeby, I. Fernandes, S. H. Ashworth, *Photochem. Photobiol. Sci.* **2014**, *13*, 62-69.
- [15] P. S. Vincett, E. M. Voigt, K. E. Rieckhoff, *J. Chem. Phys.* **1971**, *55*, 4131-4140.
- [16] a) J. R. Starkey, A. K. Rebane, M. A. Drobizhev, F. Meng, A. Gong, A. Elliott, K. McInnerney, C. W. Spangler, *Clin. Cancer Res.* **2008**, *14*, 6564-6573; b) H. A. Collins, M. Khurana, E. H. Moriyama, A. Mariampillai, E. Dahlstedt, M. Balaz, M. K. Kuimova, M. Drobizhev, V. X. D. Yang, D. Phillips, A. Rebane, B. C. Wilson, H. L. Anderson, *Nat. Photon.* **2008**, *2*, 420-424.
- [17] a) Z. Zhao, P.-S. Chan, H. Li, K.-L. Wong, R. N. S. Wong, N.-K. Mak, J. Zhang, H.-L. Tam, W.-Y. Wong, D. W. J. Kwong, W.-K. Wong, *Inorg. Chem.* **2012**, *51*, 812-821; b) B. S. Wang, J. Wang, J.-Y. Chen, *J. Mater. Chem. B* **2014**, *2*, 1594-1602; c) C. Mauriello-Jimenez, M. Henry, D. Aggad, L. Raehm, X. Cattoën, M. Wong Chi Man, C. Charnay, S. Alpugan, V. Ahsen, D. K. Tarakci, P. Maillard, M. Maynadier, M. Garcia, F. Dumoulin, M. Gary-Bobo, J.-L. Coll, V. Josserand, J.-O. Durand, *Nanoscale* **2017**, *9*, 16622-16626; d) G. Ekiner, C. Nguyen, S. Bayır, S. Dominguez Gil, Ü. İşci, M. Daurat, A. Godefroy, L. Raehm, C. Charnay, E. Oliviero, V. Ahsen, M. Gary-Bobo, J.-O. Durand, F. Dumoulin, *Chem. Commun.* **2019**, *55*, 11619-11622.
- [18] M. Khurana, H. A. Collins, A. Karotki, H. L. Anderson, D. T. Cramb, B. C. Wilson, *Photochem. Photobiol.* **2007**, *83*, 1441.
- [19] a) M. Drobizhev, N. S. Makarov, Y. Stepanenko, A. Rebane, *J. Chem. Phys.* **2006**, *124*, 224701; b) N. S. Makarov, M. Drobizhev, A. Rebane, *Opt. Express* **2008**, *16*, 4029-4047; c) M. Drobizhev, N. S. Makarov, A. Rebane, G. de la Torre, T. Torres, *J.*

- Phys. Chem. C* **2008**, *112*, 848-859; d) N. Venkatram, D. Narayana Rao, L. Giribabu, S. Venugopal Rao, *Chem. Phys. Lett.* **2008**, *464*, 211-215; e) Y. Mir, J. E. van Lier, J.-F. Allard, D. Morris, D. Houde, *Photochem. Photobiol. Sci.* **2009**, *8*, 391-395; f) M. Morisue, K. Ogawa, K. Kamada, K. Ohta, Y. Kobuke, *Chem. Commun*, **2010**, *46*, 2121-2123; g) Z. Liu, X. Xiong, Y. Li, S. Li, J. Qin, *Photochem. Photobiol. Sci.* **2011**, *10*, 1804-1809; h) M. Louzada, J. Britton, T. Nyokong, S. Khene, *J. Phys. Chem. A* **2017**, *121*, 7165-7175; i) S. Bhattacharya, C. Biswas, S. S. K. Raavi, J. Venkata Suman Krishna, N. Vamsi Krishna, L. Giribabu, V. R. Soma, *J. Phys. Chem. C* **2019**, *123*, 11118-11133; j) S. Abid, S. Ben Hassine, N. Richy, F. Camerel, B. Jamoussi, M. Blanchard-Desce, O. Mongin, F. Paul, C. O. Paul-Roth, *Molecules* **2020**, *25*, 239.
- [20] a) O. Mongin, V. Hugues, M. Blanchard-Desce, A. Merhi, S. Drouet, D. Yao, C. Paul-Roth, *Chem. Phys. Lett.* **2015**, *625*, 151-156; b) D. Yao, X. Zhang, O. Mongin, F. Paul, C. O. Paul-Roth, *Chem. Eur. J.* **2016**, *22*, 5583-5597; c) D. Yao, X. Zhang, A. Triadon, N. Richy, O. Mongin, M. Blanchard-Desce, F. Paul, C. O. Paul-Roth, *Chem. Eur. J.* **2017**, *23*, 2635-2647; d) D. Yao, X. Zhang, S. Abid, L. Shi, M. Blanchard-Desce, O. Mongin, F. Paul, C. O. Paul-Roth, *New J. Chem.* **2018**, *42*, 395-401; e) X. Zhang, S. Abid, L. Shi, Z. Sun, O. Mongin, M. Blanchard-Desce, F. Paul, C. O. Paul-Roth, *Dyes Pigm.* **2018**, *153*, 248-255; f) L. Shi, C. Nguyen, M. Daurat, A. C. Dhieb, W. Smirani, M. Blanchard-Desce, M. Gary-Bobo, O. Mongin, C. Paul-Roth, F. Paul, *Chem. Commun*, **2019**, *55*, 12231-12234; g) X. Zhang, S. Ben Hassine, N. Richy, O. Mongin, M. Blanchard-Desce, F. Paul, C. O. Paul-Roth, *New J. Chem.* **2020**, *44*, 4144-4157.
- [21] S. Abid, S. Ben Hassine, Z. Sun, N. Richy, F. Camerel, B. Jamoussi, M. Blanchard-Desce, O. Mongin, F. Paul, C. O. Paul-Roth, *Macromolecules* **2021**, *54*, 6726-6744.
- [22] a) N. Hasebe, K. Suzuki, H. Horiuchi, H. Suzuki, T. Yoshihara, T. Okutsu, S. Tobita, *Anal. Chem.* **2015**, *87*, 2360-2366; b) A. P. Losev, I. M. Byteva, G. P. Gurinovich, *Chem. Phys. Lett.* **1988**, *143*, 127-129.

Highlights

- Synthesis of two water-soluble phthalocyanines: free base & Zn(II) complex
- New photosensitizers for theranostics
- Tested *in vitro* on breast cancer cells (MCF-7)
- Allow fluorescence bioimaging and photodynamic therapy (PDT)
- The free-base was shown to be more biocompatible than the Zn(II) complex

Graphical abstract



MCF-7 Cells